ACS Catalysis

Letter

pubs.acs.org/acscatalysis

Ferric Oxide-Supported Pt Subnano Clusters for Preferential Oxidation of CO in H_2-Rich Gas at Room Temperature

Botao Qiao,[†,‡] Aiqin Wang,[†] Lin Li,[†] Qingquan Lin,[†] Haisheng Wei,[†] Jingyue Liu,*[,‡] and Tao Zhang*[,†]

[†]State Key Laboratory of Catalysis, Dalian Institute of Chemical Physics, Chinese Academy Sciences, Dalian 116023, China

[‡]Department of Physics, Arizona State University, Tempe, Arizona 85287, United States

Supporting Information

ABSTRACT: Pt single atoms and small clusters were dispersed on iron oxides by a facile coprecipitation method. These catalysts, with or without calcination at elevated temperatures, show excellent activity and selectivity for preferential oxidation of CO in the H_2-rich gas. They can completely remove CO from H_2-rich gas at a wide temperature range of 20−70 °C, which renders them suitable for low-temperature applications. The reaction followed a mixture of competitive mechanism and a noncompetitive/redox mechanism. The weakened CO adsorption on small Pt clusters and atoms makes the competitive adsorption of O_2 feasible, which ensures a high activity of Pt/Fe catalysts, even calcined at elevated temperature.

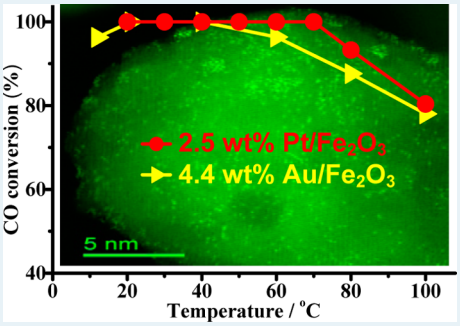

KEYWORDS: *cluster, preferential oxidation, CO, Pt, iron oxide*

Preferential oxidation of CO (PROX) has been regarded as a promising approach to reduce the CO concentration in a H_2-rich stream to an acceptable level (<50 ppm) to meet the requirement for application in proton exchange membrane fuel cells (PEMFC).[1−3] Among various catalyst formulations that have been developed to achieve this goal,[1] supported Pt catalysts are the most intensively studied and regarded as a promising candidate.[2−7] Although supported Pt catalysts have better stability and water and CO_2 resistance than the supported gold and nonnoble metal catalysts, their activity is relatively low. The commercial Pt/Al_2O_3 catalysts are active for PROX reaction only at temperatures above 200 °C.[4] Addition of promoters—for instance, Fe,[8−10] Co,[5,11,12] Cu,[13] Sn,[14] Ru,[7,15] or K,[16,17]—or use of different supports[2,6] can certainly enhance the activity for CO conversion; it is, however, difficult to realize total conversion of CO at ambient temperatures, which is particularly important for fuel cell applications in transportation.[3] In fact, there are only a few supported Pt catalysts that have shown reasonable activity for CO conversion at temperatures around 60 °C.[5−7,16] To the best of our knowledge, among all the supported Pt catalysts reported in the literature, only Pt supported by FSM-type mesoporous silica[18] and $PtFe/SiO_2$ with relatively higher Pt metal loading[19] can accomplish total conversion of CO at room temperature. Recently, we found that single Pt atoms dispersed on iron oxides could be extremely active for the PROX reaction.[20] However, because of the current limitation of the low Pt loading of the single-atom catalyst, the total conversion of CO can be realized only at a PEMFC working temperature of 80 °C. Because preparing single-atom catalyst with high loadings is—at least at this stage—a formidable challenge,[21] fabrication of supported Pt subnano cluster catalysts may provide an alternative route to maximize the Pt atom efficiency and realize a desirable PROX performance at ambient temperatures.[22]

Here, we show, for the first time, that Pt subnanometer clusters and single atoms dispersed onto iron oxide supports are highly active for the PROX reaction, with a total conversion of CO over a wide temperature window, from ambient temperature to 70 °C. We also tested an iron oxide-supported gold catalyst, a well-known highly active catalyst for CO oxidation and PROX reaction, under identical reaction conditions. Our subnanometer Pt catalysts exhibited an activity comparable to that of the gold catalysts but with a much wider temperature window for the total conversion of CO.

The Pt subnano cluster catalysts were fabricated by coprecipitation of an aqueous solution of H_2PtCl_6 and $Fe(NO_3)_3$ with an aqueous solution of Na_2CO_3 at 50 °C. The precipitate was filtered, washed, dried (denoted as Pt/Fe-UC), and calcined at 200 or 400 °C for 5 h (denoted as Pt/Fe-C2 and Pt/Fe-C4, respectively; see the support information (SI) for details). The Pt loading was 2.0 wt % for the Pt/Fe-UC catalyst (SI Table S1). The loadings for Pt/Fe-C2 and Pt/Fe-C4 were slightly higher (2.3 and 2.5 wt %, respectively), probably because of the weight loss, the phase change of the iron hydroxide during the calcination process, or both. As shown in SI Figure S1a, the iron oxide changed from amorphous for Pt/Fe-UC and Pt/Fe-C2 to typical Fe_2O_3 for Pt/Fe-C4. Together with the strutural change, the BET surface area of the corresponding catalysts decreased significantly with increasing calcination temperature (SI Table S1).

Received: April 15, 2014
Revised: May 23, 2014
Published: May 28, 2014

   dx.doi.org/10.1021/cs500501u | ACS Catal. 2014, 4, 2113−2117

SI Figure S2 shows high resolution transmission electron microscopy (HRTEM) images of Pt/Fe-UC, Pt/Fe-C2, and Pt/Fe-C4 catalysts, which had been prereduced with 10 vol % H_2/He flowing at 200 °C for 30 min. Lattice fringes with a spacing of ~0.29 nm corresponding to the (220) plane of Fe_3O_4 are clearly observed in all three samples. In addition, lattice fringes with a spacing of ~0.25 nm are also found in the Pt/Fe-C4 catalyst, which can be assigned to the (311) plane of Fe_3O_4 or the (110) plane of Fe_2O_3. Pt clusters with sizes of ~1 nm in diameter are visible in the HRTEM image of the Pt/Fe-C4 sample after being reduced in 10 vol % H_2/He. The Pt particles in the Pt/Fe-UC and Pt/Fe-C2 are not easily discernible, probably as a result of the effect of lens defocus on particle contrast[23] or that the particle sizes in these two samples are, in fact, much smaller than 1 nm in diameter.

XRD patterns (SI Figure S1b) of the reduced samples suggested that both the Pt/Fe-UC and Pt/Fe-C2 catalysts contain only Fe_3O_4 phase, whereas the Pt/Fe-C4 catalyst contains both Fe_3O_4 and Fe_2O_3 phases, in agreement with the HRTEM results. The XRD patterns did not reveal any Pt-containing crystal phases, suggesting that the Pt-containing species are highly dispersed, also in line with the HRETM results. The presence of Fe_3O_4 crystallites in the Pt/Fe catalysts indicates that the Fe^{3+} species are easily transformed to Fe^{2+}, even though the reduction treatment was relatively mild. This conclusion is further confirmed by temperature-programmed reduction with H_2 (H_2-TPR) of the three samples (SI Figure S3).

For comparison, we first performed the H_2-TPR of the pure FeO_x (ferrihydrite, as-synthesized with the same procedure but without Pt) and Fe_2O_3 (as-synthesized ferrihydrite calcined at 400 °C for 5 h) supports. The H_2-TPR profiles of both supports are composed of one sharp peak (positioned in the region of 270−340 °C, denoted as peak II) and one broad band (positioned in 400−800 °C, denoted as peak III), which corresponds to the reduction of ferrihydrite/Fe_2O_3 to Fe_3O_4 and further to FeO/Fe species, respectively.[24,25] The temperature of peak II for ferrihydrite is lower than that for Fe_2O_3, suggesting that the ferrihydrite itself is easier to reduce.[24,26] The TPR profiles for Pt/Fe-UC and Pt/Fe-C2 show an even sharper peak (peak I) at much lower temperature (110−120 °C) and a broad band (peak III). The amounts of H_2 consumption for the above two catalysts, corresponding to peak I, are 1625 and 1898 μmol g_{cat}^{-1}, respectively (SI Table S2). These are about 8-fold larger than that required for reducing Pt^{4+} to Pt^0, suggesting that the Fe^{3+} species were reduced together with the Pt^{4+} species at this temperature caused by H_2 spillover from Pt to the ferrihydrite support. On the other hand, the TPR profile of the Pt/Fe-C4 catalyst is characterized by two peaks: the peak at 90 °C can be assigned to the reduction of Pt^{4+} to Pt^0, whereas the peak centered at 222 °C is due to the partial reduction of Fe^{3+} species. It should be noted that the amount of H_2 consumption for peak I is still double that required for reducing Pt^{4+}, suggesting that some Fe^{3+} species in close contact with the Pt species were also reduced. The TPR trend of Pt/FeO_x with calcination temperature is different from the previous reported Ir/FeO_x,[22] suggesting that Pt and Ir nanoclusters interact differently with the FeO_x support.

To observe the Pt subnano clusters, we examined the Pt/Fe-C4 catalyst by an aberration-corrected scanning transmission electron microscope. Representative images of the catalyst are shown in Figure 1 and SI Figure S4. With subangstrom resolution individual Pt atoms (circles), two-dimensional Pt rafts consisting of less than 10 Pt atoms (within the diamond in the image) as well as three-dimensional Pt clusters (squires) with sizes below 1 nm were clearly observed in the HAADF images. The majority of the Pt clusters have sizes smaller than 1 nm in diameter and were uniformly dispersed onto the support (SI Figure S4a,b,c). It should be noted that no larger particles (>2 nm) were observed in low magnification images, suggesting that the catalyst sample contains only Pt nanoclusters with sizes much smaller than 2 nm in diameter. The unique properties of the iron oxides or iron hydroxides that we used might play a critical role in dispersing and stabilizing Pt nanoclusters. Even after a treatment with 400 °C calcination for 5 h and 200 °C reductions for 0.5 h, the Pt nanoclusters did not sinter much.

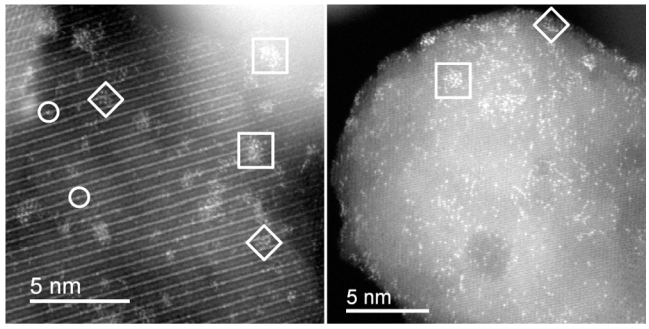

Figure 1. STEM-HAADF images of Pt/Fe-C4 sample.

The PROX reaction was tested in a fixed-bed reactor system with a continuously flowing gas mixture of 1 vol % CO, 1 vol % O_2, 40 vol % H_2, and the balance He. The space velocity was fixed at 18 750 mL g_{cat}^{-1} h^{-1}. Prior to the test, the catalyst was reduced with 10 vol % H_2/He at 200 °C for 30 min. Figure 2a shows profiles of the CO conversion as a function of the reaction temperature for the various catalysts. We also tested the 4.4 wt % Au/Fe_2O_3-WGC catalyst provided by the World Gold Council (WGC) for comparison (without any further treatment). The CO conversion reached 100% within the temperature range of 20−40 °C and then decreased gradually when the reaction temperature was further increased, consistent with the behavior of most supported Au catalysts reported in the literature.[27−30] The decrease in the CO conversion with temperature should be caused by the competitive oxidation of H_2 with O_2. Compared with the 4.4 wt % Au/Fe_2O_3-WGC catalyst, our Pt/Fe catalysts, regardless of whether calcined, were not only as active as the standard gold catalyst but also yielded 100% conversion of CO with a wider temperature window (20−70 °C). The wider temperature window for full CO conversion will provide operational flexibility in practical applications. It should be noted that the loading of Pt in our Pt/Fe catalysts is only about half that of the gold in the Au/Fe_2O_3-WGC catalyst. Even with a lower loading of Pt, for example, 0.62 wt %, the Pt/Fe-C4 catalyst still showed high activity, and 90% of CO was converted to CO_2 at 20 °C, demonstrating that our Pt/Fe catalysts are extremely active for low-temperature PROX reaction. Actually, comparing with other Pt catalysts that were reported to be very active for the PROX reaction (SI Table S3), such as Pt−Co/YSZ,[5] Pt/FSM-16,[6] Ru@Pt/Al_2O_3,[7] Pt−Fe/SiO_2,[19] and Pt−Fe/mordenite,[31] our Pt/Fe catalysts are among the best-performance ones.

To obtain the intrinsic activity of our Pt/Fe catalysts, we measured the specific rate at room temperature and calculated the corresponding turnover frequency (TOF) under a

dx.doi.org/10.1021/cs500501u | ACS Catal. 2014, 4, 2113−2117

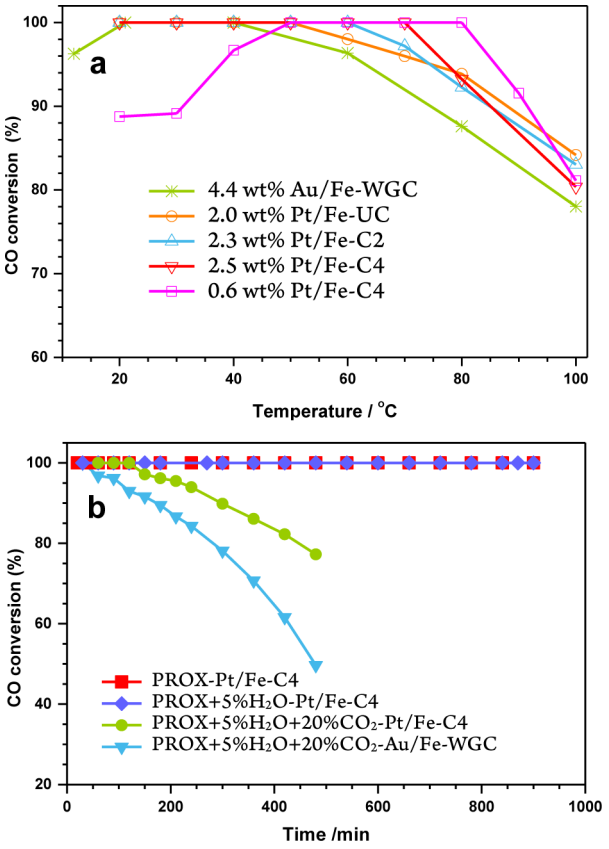

Figure 2. CO conversion as a function of (a) reaction temperature and (b) reaction time at 50 °C over various catalysts and at different reaction conditions, respectively.

differential condition (CO conversions were controlled below 20%). We also compared our data with those reported in the literature (Table 1). Clearly, all our Pt/Fe catalysts, regardless of the treatment, are highly active and have specific rates and TOFs similar to the standard Au/Fe_2O_3-WGC catalyst, suggesting that they have comparable activity when measured in per gram of gold or platinum. Compared with the Pt/Al_2O_3 catalyst, the commercially used formula for the PROX reaction, our Pt/Fe catalysts are ~100 times more active.[17] They are also several times more active than that of the alkali-promoted Pt/Al_2O_3 catalyst[16] and the Pt_3Sn/C catalyst,[14] which were both reported to be the most active Pt-based catalysts for PROX. They are only slightly less active than the recently developed Pt single-atom catalyst, with a very low loading of 0.17 wt %.[20]

Because the H_2-rich gas from reforming often contains a large amount of CO_2 and H_2O, we investigated the effect of H_2O and CO_2 on the catalytic performance of the synthesized Pt subnano cluster catalysts. As shown in Figure 2b, the presence of 5 vol % H_2O did not decrease the catalytic activity of the Pt/Fe-C4 catalyst for PROX reaction; however, further introduction of 20 vol % CO_2 in the feed stream indeed imposed a negative effect on the catalytic performance of the Pt/Fe-C4 catalyst, with CO conversion decreasing from 100% to 75% after 500 min run at 50 °C. This should be most probably due to the coverage of the active sites by CO_2 adsorption.[20] To verify this, we removed the CO_2 from the reaction mixture, as shown in SI Figure S5, and the deactivation rate decreased but the activity was not recovered, suggesting that the adsorbed CO_2 could not be removed at low temperatures (e.g., 50 °C). However, the activity completely recovered after the sample was purged with He at 200 °C for 30 min, providing evidence that the deactivation was caused by the coverage of the active sites by adsorption of CO_2. When compared to the 4.4 wt % Au/Fe_2O_3-WGC catalyst, our Pt subnano cluster catalysts still exhibited a better tolerance to CO_2 poisoning.

For CO oxidation and PROX reactions on supported Pt-group metal catalysts, the activation of O_2 is critical because the CO adsorption on these metals is so strong that O_2 cannot competitively adsorb and be activated at low temperatures.[3,22] However, it was reported recently that CO adsorption on Pt-group metal supported on partially reduced iron oxides could be significantly weakened.[32] This may enable the competitive adsorption of O_2. Furthermore, on iron oxide-supported Pt-group metal catalysts, a noncompetitive Langmuir−Hinshelwood mechanism is also plausible.[3,22] To gain more insights into the observed high activity of our Pt/Fe catalysts, we measured the CO adsorption with microcalorimetry. As shown in SI Figure S6, the microcalorimetry data shows that the initial CO adsorption heat was only ~96 kJ/mol, much lower than that of the CO adsorption on an L-zeolite supported Pt small clusters (~175 kJ/mol) and on single-crystal platinum surfaces (~180 kJ/mol).[33] This result unambiguously confirms that the CO adsorption on our Pt/Fe catalysts was so low that the competitive adsorption of O_2 on the same active sites was possible.

We further performed in situ diffuse reflectance infrared Fourier transform spectroscopy (DRIFTS) measurements under 1 vol % CO flow and then 1 vol % CO + 1 vol % O_2 flow. As shown in Figure 3, under 1 vol % CO/He gas flow, three bands centered at 2170, 2120, and 2068 cm^{-1} were

Table 1. Specific Rates and TOFs of Pt Subnano Catalysts in Comparison with Other Typical Pt Catalysts Reported in the Literatures

	Pt(Au) loadings, wt %	reaction	specific rate $\times 10^2$, $mol_{CO}\ h^{-1}\ g_{Au/Pt}^{-1}$	TOF $\times 10^2$, s^{-1}	temp, °C	note
Au/Fe_2O_3	4.4	PROX	39.3	8.6[a]	27	this work
Pt/Fe-UC	2.0	PROX	19.3	14.0[b]	27	this work
Pt/Fe-C2	2.3	PROX	25.8	18.1[b]	27	this work
Pt/Fe-C4	2.5	PROX	20.3	9.2[b]	27	this work
Pt_3Sn/C	16.6	PROX		~2.3[c]	27	ref 14
Pt/Al_2O_3	2.0	PROX		~0.2	80	ref 16
$K-Pt/Al_2O_3$[c]	2.0	PROX		~3.2	80	ref 16
Pt/Fe_2O_3	0.17	PROX	67.6	21.2	27	ref 20

[a]Gold dispersion was calculated according to the relationship between the degree of dispersion and the particle size: $D = 0.9/d_{Au}$; [b]Pt dispersion was obtained by CO chemisorption by assuming CO/Pt = 1/1. [c]Calculated on the basis of the activation energy and the TOF data at 80 °C.

dx.doi.org/10.1021/cs500501u | ACS Catal. 2014, 4, 2113−2117

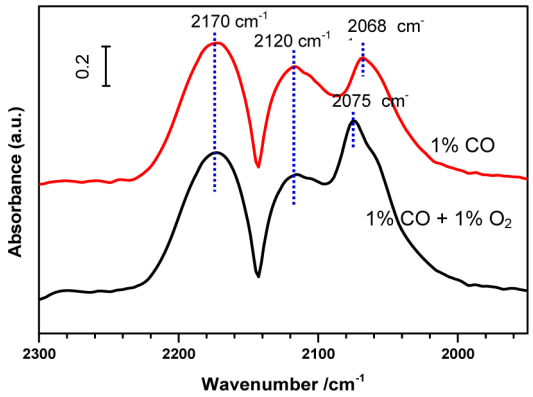

Figure 3. In situ DRIFT spectra of CO adsorption and CO + O_2 coadsorption on the Pt/Fe-C4 sample.

observed. The former two bands are attributed to the gas-phase CO (R and P branches)[34] and the last band was ascribed to the CO adsorption on metallic Pt site.[35,36] After introduction of 1 vol % O_2, the gas-phase CO bands remain unchanged. However, the band of the adsorbed CO shifted to a higher frequency of 2075 cm^{-1}. Such a shift reflects the decreased back-donation of electrons from Pt to CO, suggesting that the competitive adsorption of O_2 on the same Pt sites had occurred.[35]

This conclusion is opposite that obtained on an Ir/Fe catalyst that the CO adsorption remained unchanged after introduction of O_2,[22] suggesting that the CO oxidation on the Pt/Fe catalysts followed, at least partially, the competitive L−H mechanism. In addition, the reaction rate shows that after calcination at 400 °C, the TOF of the Pt/Fe catalysts decreased to half. This suggested that the CO oxidation on the Pt/Fe catalysts also followed a noncompetitive L−H mechanism[22] or a redox mechanism[20,26] because if it completely followed the competitive L−H mechanism, the reaction data should be similar. Furthermore, for the noncompetitive L−H or redox mechanism, the activation of O_2 occurred on the FeO_x support. Because the ability of FeO_x support to activate O_2 decreased seriously after calcination at 400 °C,[22,26] the activity of Pt/Fe-C4 would accordingly decrease if they followed a noncompetitive or redox mechanism, which is very consistent with the experimental data. Clearly, from these characterization data and analysis, we can conclude that the CO oxidation followed a mixture of competitive L−H mechanism and a noncompetitive LH/redox mechanism. The competitive L−H mechanism ensures that the activity of high-temperature calcined Pt/Fe-C4 sample was high enough.

In summary, we have synthesized uniformly dispersed Pt subnano clusters and single atoms on iron oxide supports by a facile coprecipitation method. Compared with the standard Au/Fe_2O_3-WGC catalyst, our Pt/Fe catalysts, with or without calcination at elevated temperatures, exhibited a comparable activity but a wider temperature window for CO total conversion and a better tolerance to CO_2 poisoning. The reaction followed a mixture of competitive mechanism and a noncompetitive/redox mechanism. The weakened CO adsorption on small Pt clusters and atoms makes the competitive adsorption of O_2 feasible, which ensures a high activity of Pt/Fe catalysts, even calcined at elevated temperature. The highly dispersed Pt single atoms and subnano clusters increase the atom efficiency of Pt metal. The realization of CO total conversation at ambient temperatures with a wide temperature range makes these catalysts more applicable for the PROX reaction.

■ ASSOCIATED CONTENT

Supporting Information

Details for catalyst preparation, PROX performance test, catalyst characterization, physiochemical properties, XRD, HRTEM, H_2-TPR, STEM-HAADF, microcalorimetry. This material is available free of charge via the Internet at http://pubs.acs.org."

■ AUTHOR INFORMATION

Corresponding Authors

*E-mail: Jingyue.Liu@asu.edu.
*E-mail: taozhang@dicp.ac.cn.

Notes

The authors declare no competing financial interest.

■ ACKNOWLEDGMENTS

This work was financially supported by National Nature Science Foundation of China (21173218, 21277140, 21303184) and Arizona State University. J. Liu acknowledges the start-up fund of the College of Liberal Arts and Sciences of Arizona State University and the use of facilities in the John M. Cowley Center for High Resolution Electron Microscopy at Arizona State University.

■ REFERENCES

(1) Park, E. D.; Lee, D.; Lee, H. C. *Catal. Today* **2009**, *139*, 280−290.
(2) Huang, S.; Hara, K.; Fukuoka, A. *Engergy Environ. Sci.* **2009**, *2*, 1060−1068.
(3) Liu, K.; Wang, A. Q.; Zhang, T. *ACS Catal.* **2012**, *2*, 1165−1178.
(4) Oh, S. H.; Sinkevitch, R. M. *J. Catal.* **1993**, *142*, 254−262.
(5) Ko, E. Y.; Park, E. D.; Lee, H. C.; Lee, D.; Kim, S. *Angew. Chem., Int. Ed.* **2007**, *46*, 734−737.
(6) Fukuoka, A.; Kimura, J.-i.; Oshio, T.; Sakamoto, Y.; Ichikawa, M. *J. Am. Chem. Soc.* **2007**, *129*, 10120−10125.
(7) Alayoglu, S.; Nilekar, A. U.; Mavrikakis, M.; Eichhorn, B. *Nat. Mater.* **2008**, *7*, 333−338.
(8) Liu, X.; Korotkikh, O.; Farrauto, R. *Appl. Catal., A* **2002**, *226*, 293−303.
(9) Kotobuki, M.; Watanabe, A.; Uchida, H.; Yamashita, H.; Watanabe, M. *J. Catal.* **2005**, *236*, 262−269.
(10) Sirijaruphan, A.; Goodwin, J. G.; Rice, R. W. *J. Catal.* **2004**, *224*, 304−313.
(11) Epling, W. S.; Cheekatamarla, P. K.; Lane, A. M. *Chem. Eng. J.* **2003**, *93*, 61−68.
(12) Choi, J.; Shin, C. B.; Suh, D. J. *Catal. Commun.* **2008**, *9*, 880−885.
(13) Komatsu, T.; Tamura, A. *J. Catal.* **2008**, *258*, 306−314.
(14) Schubert, M. M.; Kahlich, M. J.; Feldmeyer, G.; Huttner, M.; Hackenberg, S.; Gasteiger, H. A.; Behm, R. J. *Phys. Chem. Chem. Phys.* **2001**, *3*, 1123−1131.
(15) Chin, S. Y.; Alexeev, O. S.; Amiridis, M. D. *J. Catal.* **2006**, *243*, 329−339.
(16) Minemura, Y.; Ito, S.-i.; Miyao, T.; Naito, S.; Tomishige, K.; Kunimori, K. *Chem. Commun.* **2005**, 1429−1431.
(17) Kuriyama, M.; Tanaka, H.; Ito, S.-i.; Kubota, T.; Miyao, T.; Naito, S.; Tomishige, K.; Kunimori, K. *J. Catal.* **2007**, *252*, 39−48.
(18) Huang, S.; Hara, K.; Okubo, Y.; Yanagi, M.; Nambu, H.; Fukuoka, A. *Appl. Catal., A* **2009**, *365*, 268−273.
(19) Fu, Q.; Li, W.-X.; Yao, Y.; Liu, H.; Su, H.-Y.; Ma, D.; Gu, X.-K.; Chen, L.; Wang, Z.; Zhang, H.; Wang, B.; Bao, X. *Science* **2010**, *328*, 1141−1144.
(20) Qiao, B.; Wang, A.; Yang, X.; Allard, L. F.; Jiang, Z.; Cui, Y.; Liu, J.; Li, J.; Zhang, T. *Nat. Chem.* **2011**, *3*, 634−641.

(21) Yang, X.-F.; Wang, A.; Qiao, B.; Li, J.; Liu, J.; Zhang, T. *Acc. Chem. Res.* **2013**, *46*, 1740−1748.
(22) Lin, J.; Qiao, B.; Liu, J.; Huang, Y.; Wang, A.; Li, L.; Zhang, W.; Allard, L. F.; Wang, X.; Zhang, T. *Angew. Chem., Int. Ed.* **2012**, *51*, 2920−2924.
(23) Liu, J. *ChemCatChem.* **2011**, *3*, 934−948.
(24) Li, P.; Miser, D. E.; Rabiei, S.; Yadav, R. T.; Hajaligol, M. R. *Appl. Catal., B* **2003**, *43*, 151−162.
(25) Zielinski, J.; Zglinicka, I.; Znak, L.; Kaszkur, Z. *Appl. Catal., A* **2010**, *381*, 191−196.
(26) Li, L.; Wang, A.; Qiao, B.; Lin, J.; Huang, Y.; Wang, X.; Zhang, T. *J. Catal.* **2013**, *299*, 90−100.
(27) Qiao, B.; Zhang, J.; Liu, L.; Deng, Y. *Appl. Catal., A* **2008**, *340*, 220−228.
(28) Imai, H.; Date, M.; Tsubota, S. *Catal. Lett.* **2008**, *124*, 68−73.
(29) Schubert, M. M.; Venugopal, A.; Kahlich, M. J.; Plzak, V.; Behm, R. J. *J. Catal.* **2004**, *222*, 32−40.
(30) Avgouropoulos, G.; Ioannides, T.; Papadopoulou, C.; Batista, J.; Hocevar, S.; Matralis, H. K. *Catal. Today* **2002**, *75*, 157−167.
(31) Watanabe, M.; Uchida, H.; Ohkubo, K.; Igarashi, H. *Appl. Catal., B* **2003**, *46*, 595−600.
(32) Xiao, C.; Liang, M.; Gao, A.; Xie, J.; Wang, Y.; Liu, H. *J. Nanopart. Res.* **2013**, *15*, 1−11.
(33) Watwe, R. M.; Spiewak, B. E.; Cortright, R. D.; Dumesic, J. A. *Catal. Lett.* **1998**, *51*, 139−147.
(34) McQuire, M. W.; Rochester, C. H.; Anderson, J. A. *J. Chem. Soc., Faraday Trans.* **1992**, *88*, 879−886.
(35) Hadjiivanov, K. I.; Vayssilov, G. N. *Adv. Catal.* **2002**, *47*, 307−511.
(36) Sonström, P.; Arndt, D.; Wang, X.; Zielasek, V.; Bäumer, M. *Angew. Chem., Int. Ed.* **2011**, *50*, 3888−3891.